Joule

CellPress

Article

Electrocatalytic Rate Alignment Enhances Syngas Generation

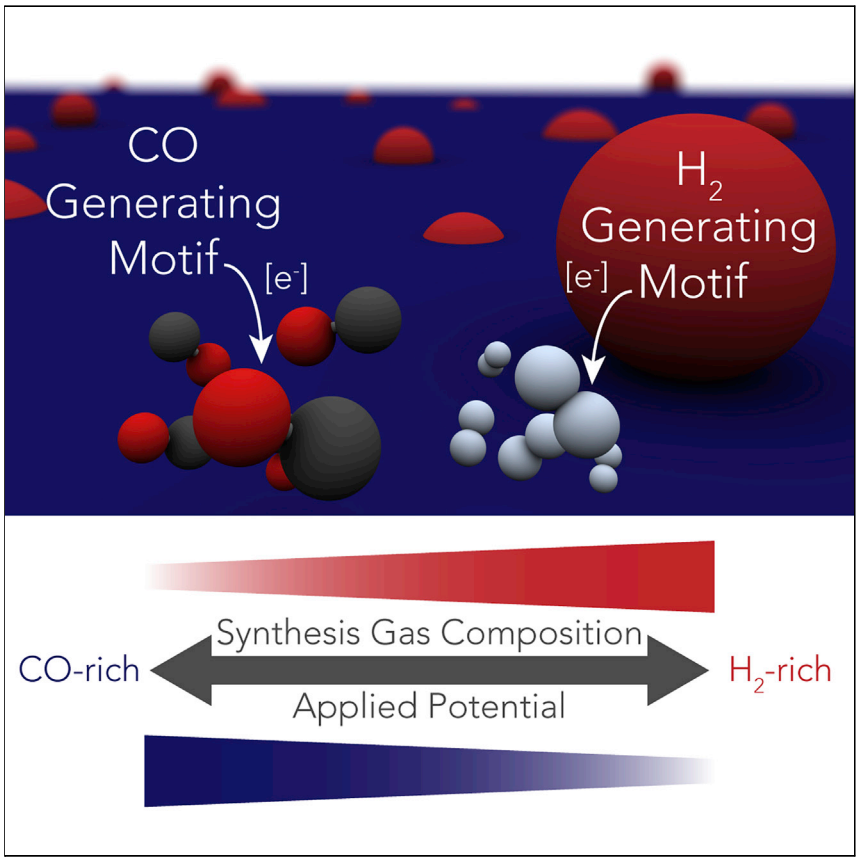

A rate-aligned electrocatalyst is reported that provides tunable access to a range of synthesis gas compositions as a function of potential. These electrocatalysts comprise a Au CO-generating component and a Co, Fe, or Ni H_2-generating component. The orthogonal integration of these two materials enhances the ability to tune syngas ratio, such that a wide range of desirable syngas compositions are accessed over a narrow potential range, all at high geometric current densities.

Michael B. Ross, Yifan Li, Phil De Luna, Dohyung Kim, Edward H. Sargent, Peidong Yang

ted.sargent@utoronto.ca (E.H.S.)
p_yang@berkeley.edu (P.Y.)

HIGHLIGHTS

CO- and H_2-generating motifs are integrated to create rate-aligned electrocatalysts

Rate-aligned electrocatalysts controllably access a range of synthesis gas mixtures

Desirable synthesis gas mixtures are made at current densities greater than 50 mA/cm^2

Ross et al., Joule 3, 1–8
January 16, 2019
https://doi.org/10.1016/j.joule.2018.09.013

Please cite this article in press as: Ross et al., Electrocatalytic Rate Alignment Enhances Syngas Generation, Joule (2018), https://doi.org/10.1016/j.joule.2018.09.013

Joule

CellPress

Article

Electrocatalytic Rate Alignment Enhances Syngas Generation

Michael B. Ross,[1,2] Yifan Li,[1,3] Phil De Luna,[2,4] Dohyung Kim,[5] Edward H. Sargent,[2,6,*] and Peidong Yang[1,2,3,5,7,8,*]

SUMMARY

Electrocatalytically generating synthesis gas (syngas, CO + H_2) from aqueous CO_2 requires balancing the relative rates of CO and H_2 generation such that the needed range of desired syngas compositions can be achieved. By purposely integrating two distinct catalytic materials, one for H_2 generation and one for CO generation, we deliberately aligned the rates of these two reactions, thereby enhancing syngas tunability as a function of potential. A modular synthetic approach enabled the systematic surface decoration of Au nanostructured electrocatalysts with a series of 3d transition metals, Co, Ni, and Fe, which augmented the selective CO generation of the Au substrate with rapid H_2 generation. The resulting rate-aligned electrocatalyst generates—in contrast with the non-rate-aligned control—a wide range of desirable syngas compositions over a 200 mV range, all at current densities greater than 50 mA/cm^2.

INTRODUCTION

The ability to convert CO_2 into chemicals provides a synthetic route to chemical fuels and feedstocks that does not rely on fossil fuels.[1,2] Catalyzing the CO_2 reduction reaction (CO_2RR) electrochemically makes use of increasingly abundant and low-cost renewable electricity.[3]

Synthesis gas (syngas), a mixture of H_2 and CO, can be converted to a variety of fuels and chemicals using established industrial processes.[4–6] These processes require different syngas compositions, and thus demand generation of both CO-rich and H_2-rich mixtures—typically ranging from 0.3–4.0 H_2:CO—at high current densities.[6–8] Generating different syngas compositions with a single electrocatalyst could provide a versatile and modular approach to producing syngas, compared with the case of separate CO and H_2 generation, which requires capital-intensive mixing and separation infrastructure that is less amenable to on-site or small-scale production.[9] Furthermore, a single tunable electrocatalyst that provides dynamic control over syngas composition would enable real-time optimization according to downstream reaction needs, e.g., varying reactor conditions.[6,8]

If syngas compositional tuning could instead be accomplished over a narrow potential window, the energy efficiency of the generation process could be kept high as the syngas composition is modified; whereas in an electrocatalyst with poor syngas tunability, large changes in potential would be required to achieve the same compositions, reducing energy efficiency.[10]

Most syngas-generating electrocatalysts use a single material that does not provide simultaneous, balanced, high CO_2RR and hydrogen evolution reaction (HER)

Context & Scale

Using renewable energy to create necessary fuels, chemicals, and fertilizers provides an attractive approach to lessen societal dependence on fossil fuels. Using CO_2 as a feedstock in this process would lower net emissions into the atmosphere, effectively recycling CO_2. Converting CO_2 and water into synthesis gas, a mixture of CO and H_2, is desirable because synthesis gas is a precursor that can be used in downstream processes to make fuels and chemicals. Importantly, each of these processes requires a different ratio of CO and H_2.

Here, we report a material that can controllably access a range of synthesis gas compositions at high reaction rates and with reasonable energy efficiency. This material was created by integrating two materials, Au to generate CO and Co, Fe, or Ni to generate H_2. This enhanced functionality brought about through material integration provides an exciting approach for creating new classes of materials that can synthesize chemicals using electrical energy.

Joule

CellPress

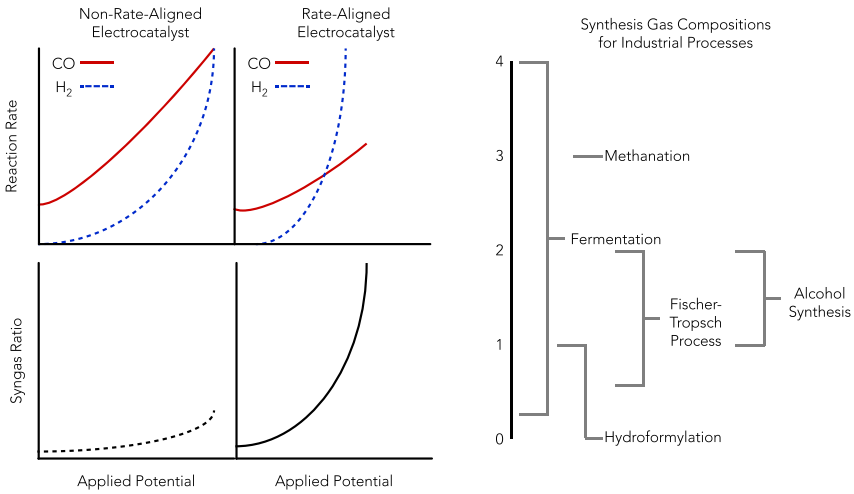

Figure 1. Rate-Aligned Electrocatalysts for Syngas Generation

Rate alignment for enhanced syngas generation. The top plots depict the relative rates of CO (red solid traces) and H_2 (blue dashed traces) generation, and the bottom plots depict how a rate-aligned electrocatalyst will access a wider range of syngas compositions over a narrow potential window. The right panel highlights common industrial syngas compositions.

activity.[8] In contrast, an electrocatalyst that uses two orthogonal reaction sites, one for CO_2RR and one for HER, could controllably align the relative rates of CO and H_2 generation to achieve tunable access to different syngas compositions. This alignment would occur because the potential-dependent behavior of the two reaction sites is decoupled by virtue of their distinct material properties. This strategy could provide access to a wide range of syngas compositions over a narrow potential window—and thus at similarly attractive energy conversion efficiencies—while maintaining or increasing current densities compared with other strategies for tuning syngas composition.[9,11–14] This approach requires that the two sites operate efficiently under similar conditions.

Here, we introduce the concept of electrocatalytic rate alignment using bifunctional electrocatalysts that generate synthesis gas from aqueous CO_2 (Figure 1). Conceptually, electrocatalytic rate alignment can be first considered by averaging the combination of two distinct electrocatalytic materials, one for CO_2RR (Au foil) and one for HER (Co foil) (Figure S1, simulated rate alignment Figure 2). However, to achieve meaningful current densities and to obviate the need to synthesize and optimize multiple syntheses for different catalytic materials, we developed a modular electrochemical synthesis to access compositionally distinct rate-aligned electrocatalysts. These nanostructured electrocatalysts interface two materials: Au for CO production and a first-row transition metal (Co, Ni, or Fe) for H_2 production. As a result of rate alignment, these electrocatalysts generate a wider range of syngas compositions over a given potential window than a bare, non-rate-aligned electrocatalyst (Tables S1–S3). Over a 200 mV window, the bare Au electrocatalyst only accesses syngas ratios from 0.2 to 0.5, while the Co rate-aligned electrocatalyst accesses ratios of 0.6–2.3. These are accessed at current densities greater than 50 mA/cm^2 for CO-rich syngas mixtures, and at current densities greater than 150 mA/cm^2 for the H_2-rich syngas mixtures (Figure 2). Electrocatalysts rate aligned with Fe and Ni access synthesis gas ratios of 0.5–3.8 and 0.3–2.1, respectively, albeit at a more negative potential window than with Co.

[1]Department of Chemistry, University of California, Berkeley, Berkeley, CA 94720, USA

[2]Bio-Inspired Solar Energy Program, Canadian Institute for Advanced Research, Toronto, ON M5G 1Z8, Canada

[3]Chemical Sciences Division, Lawrence Berkeley National Laboratory, Berkeley, CA 94720, USA

[4]Department of Materials Science and Engineering, University of Toronto, Toronto, ON M5S 3E4, Canada

[5]Department of Materials Science and Engineering, University of California, Berkeley, Berkeley, CA 94720, USA

[6]Department of Electrical and Computer Engineering, University of Toronto, Toronto, ON M5S 3G4, Canada

[7]Kavli Energy Nanoscience Institute, University of California, Berkeley, Berkeley, CA 94720, USA

[8]Lead Contact

*Correspondence: ted.sargent@utoronto.ca (E.H.S.), p_yang@berkeley.edu (P.Y.)

https://doi.org/10.1016/j.joule.2018.09.013

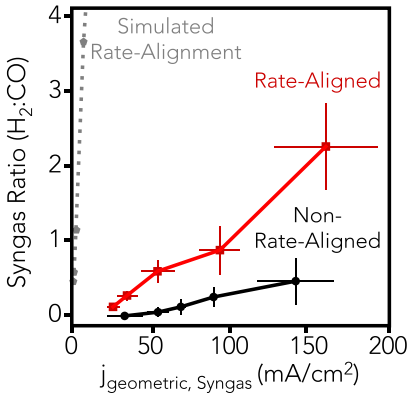

Figure 2. Geometric Current Densities and Syngas Tunability Achieved through Rate Alignment

Simulated co-electrolysis with Au and Co polycrystalline foils (gray dashed trace), non-rate-aligned Au nanostructure electrocatalyst (black circles), and Co rate-aligned nanostructured electrocatalyst (red squares). The mean and one standard deviation are calculated from three separately prepared samples.

RESULTS

Theory-Informed Design of Two-Component Rate-Aligned Electrocatalysts

Density functional theory (DFT) calculations and literature precedent were used to identify metals that could enable rate alignment (see Experimental Procedures, Tables S4–S7). Previous experimental and theoretical work suggests that Au is effective for CO generation, particularly when nanostructured.[3,15] Fe, Ni, and Co were chosen as the second component due to their more rapid HER kinetics than Au[3,16] in addition to their structural preference for segregation, which should minimize mixing between the two components.[17,18] Thermodynamic calculations along the CO_2RR (Figures 3B) and HER (3C) pathways on both low- (Figures 3B and 3C) and high-energy surfaces (Figure S2) support that Au binds the rate-determining intermediate for CO_2RR (*COOH) more optimally, while the 3d transition metals bind the rate-determining HER intermediate (H*) more optimally.[3,16,19–21] Thus, we set out to controllably interface these metals.

Rate-aligned electrocatalysts were synthesized electrochemically using a two-step process where the first step creates a layer of Zn across the surface and the second step exchanges that templated Zn layer for the metal of interest. This two-step procedure provides a rapid method to deposit a second metal onto the Au surface without the need for element-specific procedures. Zn was electrodeposited[22] (Figure S3) on Au nanostructured electrocatalysts that synthesize CO with high current densities at relatively low overpotential.[15] Successful deposition was confirmed using X-ray photoelectron spectroscopy and X-ray absorption spectroscopy (XAS, Figure S4). Next, the Zn atoms were galvanically exchanged with the more noble metal cation (see Experimental Procedures).[23] While the aqueous environment likely induces restructuring of the deposited metal and some corrosion of the Zn, this approach enabled consistent deposition of Co, Ni, and Fe. Comparison of the relative X-ray absorption intensities suggests that similar amounts of these transition metals are present after exchange (Figure S5). Post-synthetic stripping of Co reveals ~1 μg/cm^2 after one deposition cycle, and that iterative deposition can be used to increase the loading of the secondary transition metal (Table S8).[23]

Structural and Spectroscopic Characterization Confirm Synthesis of Two-Component Electrocatalysts

Electron microscopy was used to characterize further the structure of the rate-aligned electrocatalysts. Zn deposition was not observed to perturb the nanoscale

Please cite this article in press as: Ross et al., Electrocatalytic Rate Alignment Enhances Syngas Generation, Joule (2018), https://doi.org/10.1016/j.joule.2018.09.013

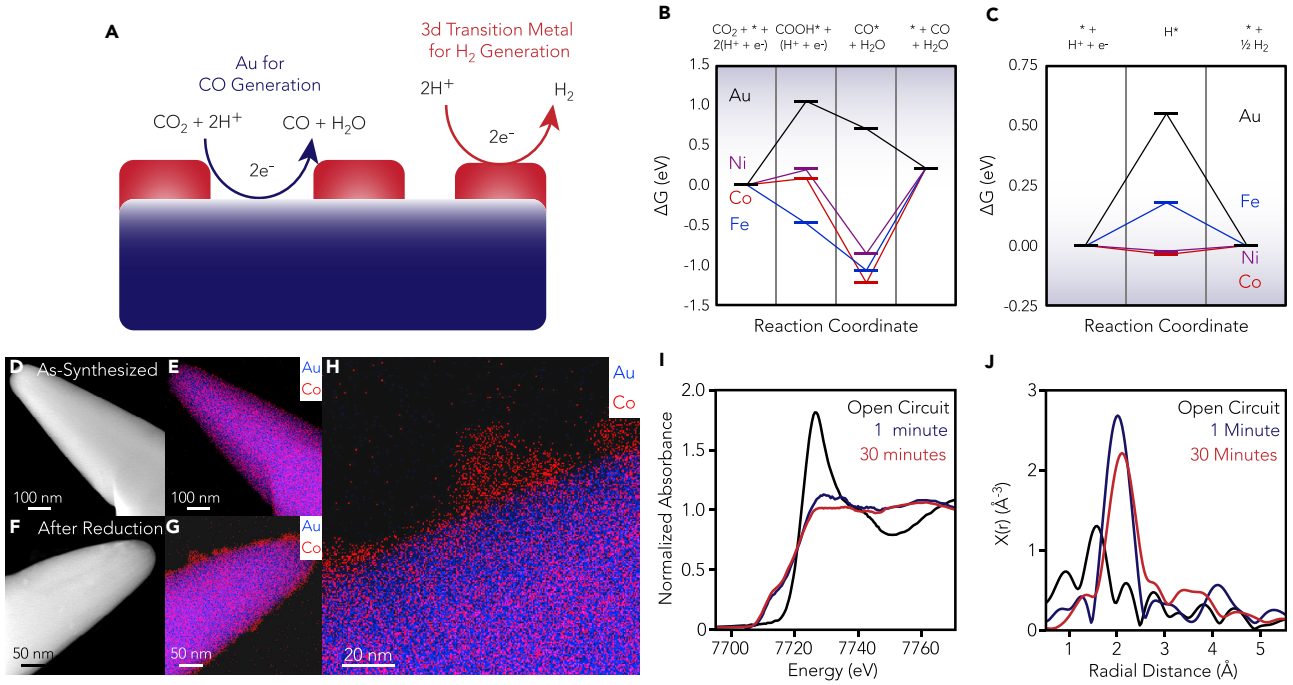

Figure 3. Design and Synthesis of a Multi-Component Rate-Aligned Electrocatalyst

(A) Scheme of a two-site catalytic surface.

(B and C) DFT calculations that compare the thermodynamics of CO (B) and H_2 (C) generation on the low energy surfaces of Au (black), Co (red), Ni (purple), and Fe (blue).

(D–G) High-angle annular dark-field scanning transmission electron micrograph (D) and corresponding energy dispersive X-ray spectroscopic mapping of Au and Co (E) of the as-synthesized electrocatalyst. High-angle annular dark-field scanning transmission electron micrograph (F) and corresponding energy dispersive X-ray spectroscopic mapping of Au and Co (G) of the electrocatalyst after reduction at −0.8 V versus RHE.

(H) Energy dispersive X-ray spectroscopic mapping of Au and Co at the catalyst surface after reduction.

(I) *In situ* X-ray absorption spectra of the Co rate-aligned electrocatalyst at open circuit (black), at −1.0 V versus RHE after 1 min (blue) and 30 min (red).

(J) The apparent radial atomic coordination environments under the same conditions.

or microscale structure of the Au electrode (Figure S6). Scanning transmission electron microscopy-coupled energy-dispersive X-ray spectroscopy (EDS) mapping shows that Co is well dispersed across the surface at the tens-of-nanometer scale (Figures 3D and 3E), while analogous characterization after electrocatalysis reveals that Co remains on the surface after reduction in CO_2RR conditions (Figures 3F–3H and S7). Finally, EDS does not indicate that Zn is present after replacement by Co (Figure S8).

To understand the structure of the Co electrocatalyst under working electrochemical conditions, we used *in situ* XAS to probe Co at the K-edge.[24] Specifically, X-ray absorption near edge structure (XANES) analysis probed the oxidation state while extended X-ray absorption fine structure (EXAFS) analysis probed the Co coordination environment. *In situ* XANES spectra qualitatively show that the Co is at least partly oxidized at open-circuit conditions (immersed in 0.1 M $KHCO_3$ electrolyte), whereas at −1.0 V versus reversible hydrogen electrode (RHE), it is reduced rapidly (under 1 min) and remains reduced (measured up to 30 min) (Figure 3I).[24,25] Analysis of the EXAFS region (see Experimental Procedures) provides a radial distribution function that describes the coordination environment around Co (Figure 3J). The apparent average bond length increases upon reduction, from 1.56 Å at open circuit to 2.00 Å and 2.09 Å at 1 min and 30 min at −1.0 V versus RHE, respectively. This is consistent with conversion from a Co-O dominant species to a Co-Co dominant species.[24]

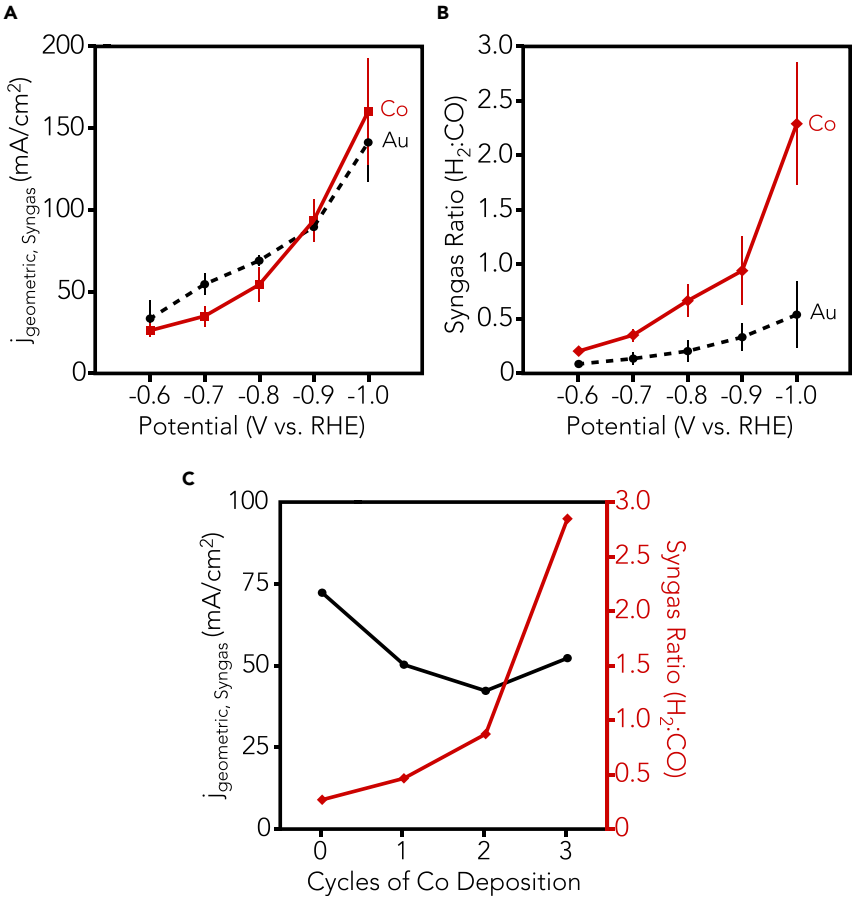

Figure 4. Realization of a Nanostructured Co Rate-Aligned Electrocatalyst

(A) Geometric current density toward syngas for the Co rate-aligned (red) and bare Au (black) electrocatalysts. The mean and one standard deviation are calculated from three separately prepared samples.

(B) Syngas ratios for the same.

(C) Syngas generation with electrocatalysts modified with 0, 1, 2, and 3 cycles of Co surface deposition (electrocatalysis at −0.8 V versus RHE).

Rate Alignment Improves the Potential-Dependent Tunability of Syngas Composition

Electrocatalysis in CO_2-saturated 0.1 M $KHCO_3$ revealed that the geometric current density of the rate-aligned electrocatalyst is within 10% of the bare Au one (Figure 4A, red solid and black solid curves, Figure S9), while the range of accessible syngas ratios is wider for the rate-aligned electrocatalyst (Figure 4B and Table 1). Thus, the Co rate-aligned electrocatalyst provides access to a broader range of syngas compositions at a lower overpotential than the bare Au electrocatalyst, i.e., it can synthesize them more energy efficiently. Finally, the rate-aligned electrocatalyst exhibits reasonable stability at longer working times (Figure S10).

To explore the bifunctional nature of the rate-aligned electrocatalyst, we cycled the two-step synthetic approach to deposit Co multiple times on the electrocatalyst surface (Table S8). A monotonic relationship was observed between the number of Co deposition cycles and the syngas ratio at the same applied potential (−0.8 V versus RHE), providing further evidence for rate alignment enabled by bifunctionality (Figure 4C). Specifically, increasing the number of Co deposition cycles increased the

Table 1. Quantification of Syngas Ratio Rate Alignment

	Potential Window (V versus RHE)	Accessible Syngas Range
Co rate-aligned	−0.8 to −1.0	0.62–2.27
	−0.7 to −1.0	0.30–2.27
Bare Au non-rate-aligned	−0.8 to −1.0	0.15–0.49
	−0.7 to −1.0	0.08–0.49

rate of H_2 generation while decreasing the rate of CO generation, resulting in an overall increase in the syngas ratio when compared at the same potential.

Both Fe and Ni also increase the potential-dependent sensitivity of the syngas ratio compared with the bare Au electrocatalyst, although more negative potentials are required to access the H_2-rich compositions (Figures S11 and S12). While the bare Au electrocatalyst accesses a range of 0.3–0.6 over a 200 mV range (−0.9 to −1.1 V versus RHE), the rate-aligned electrocatalysts all exhibit broader syngas tunability, with Fe accessing 0.5–3.8 and Ni accessing 0.3–2.1 (over the same potential range, Table S1).

DISCUSSION

We have described electrocatalytic rate alignment as an approach to enhance synthesis gas (CO and H_2) generation from aqueous CO_2. Development of a modular synthetic approach for decorating a high surface area Au electrocatalyst with 3d transition metals enabled the investigation of two-component, rate-aligned electrocatalysts. The enhanced potential sensitivity of syngas composition of these electrocatalysts is coupled with high current densities, ranging from 50 mA/cm^2 for CO-rich syngas mixtures to 150–180 mA/cm^2 for H_2-rich ones.

Further exploration of integrated CO- and H_2-generating catalytic motifs could improve this concept of rate alignment for syngas production, providing reductions in overpotential and increases in current density that are essential for commercial progress.[6,10] Future investigation into competitive or cooperative interactions between distinct electrocatalyst components in close proximity is also of interest. Integration with state-of-the-art electrolyzer technology would facilitate translation to full-cell electrocatalytic architectures.[26,27] Finally, the ability to access different synthesis gas compositions further enables the direct integration with downstream industrial processes that utilize syngas, potentially with real-time control over composition to adjust to variable reactor conditions.[5,8]

EXPERIMENTAL PROCEDURES

Detailed Experimental Procedures can be found in the Supplemental Information.

SUPPLEMENTAL INFORMATION

Supplemental Information includes Supplemental Experimental Procedures, 12 figures, and 8 tables and can be found with this article online at https://doi.org/10.1016/j.joule.2018.09.013.

ACKNOWLEDGMENTS

This work was supported by the CIFAR Bio-Inspired Solar Energy Program and by the Director, Office of Science, Office of Basic Energy Sciences, Chemical Sciences, Geosciences, and Biosciences Division, of the U.S. Department of Energy under contract no. DE-AC02-05CH11231 within the Catalysis Research Program (FWP no.

CH030201). XAS data were collected at the Soft X-ray Microcharacterization Beamline (SXRMB) at the Canadian Light Source with the assistance of Dr. Yongfeng Hu. Work at the Molecular Foundry was supported by the Office of Science, Office of Basic Energy Sciences, of the U.S. Department of Energy under contract no. DE-AC02-05CH11231. Calculations were performed on the SOSCIP Consortium's Blue Gene/Q computing platform. SOSCIP is funded by the Federal Economic Development Agency of Southern Ontario, the Province of Ontario, IBM Canada Ltd., Ontario Centres of Excellence, Mitacs, and 15 Ontario academic member institutions. M.B.R. gratefully acknowledges support from the CIFAR Bio-Inspired Solar Energy Program (Postdoctoral Fellowship). P.D.L. wishes to thank the Natural Sciences and Engineering Research Council (NSERC) of Canada for support in the form of the Canadian Graduate Scholarship – Doctoral award. D.K. acknowledges support from Samsung Scholarship.

AUTHOR CONTRIBUTIONS

M.B.R. designed the systems, collected and analyzed data, and wrote the manuscript. Y.L., P.D.L., and D.K. collected and analyzed data and wrote the manuscript. E.H.S. and P.Y. designed the systems, analyzed the data, and wrote the manuscript.

DECLARATION OF INTERESTS

The authors declare no competing interests.

Received: June 12, 2018
Revised: August 17, 2018
Accepted: September 14, 2018
Published: October 9, 2018

REFERENCES

1. Chu, S., Cui, Y., and Liu, N. (2016). The path towards sustainable energy. Nat. Mater. *16*, 16–22.

2. Kim, D., Sakimoto, K.K., Hong, D., and Yang, P. (2015). Artificial photosynthesis for sustainable fuel and chemical production. Angew. Chem. Int. Ed. *54*, 3259–3266.

3. She, Z.W., Kibsgaard, J., Dickens, C.F., Chorkendorff, I., Nørskov, J.K., and Jaramillo, T.F. (2017). Combining theory and experiment in electrocatalysis: insights into materials design. Science *355*, eaad4998.

4. Jhong, H.R.M., Ma, S., and Kenis, P.J. (2013). Electrochemical conversion of CO_2 to useful chemicals: current status, remaining challenges, and future opportunities. Curr. Opin. Chem. Eng. *2*, 191–199.

5. Haas, T., Krause, R., Weber, R., Demler, M., and Schmid, G. (2018). Technical photosynthesis involving CO_2 electrolysis and fermentation. Nat. Catal. *1*, 32.

6. Foit, S.R., Vinke, I.C., de Haart, L.G.J., and Eichel, R.A. (2017). Power-to-syngas: an enabling technology for the transition of the energy system? Angew. Chem. Int. Ed. *56*, 5402–5411.

7. Acharya, B., Roy, P., and Dutta, A. (2014). Review of syngas fermentation processes for bioethanol. Biofuels *5*, 551–564.

8. Hernández, S., Amin Farkhondehfal, M., Sastre, F., Makkee, M., Saracco, G., and Russo, N. (2017). Syngas production from electrochemical reduction of CO_2: current status and prospective implementation. Green Chem. *19*, 2326–2346.

9. Kumar, B., Brian, J.P., Atla, V., Kumari, S., Bertram, K.A., White, R.T., and Spurgeon, J.M. (2016). Controlling the product syngas H_2:CO ratio through pulsed-bias electrochemical reduction of CO_2 on copper. ACS Catal. *6*, 4739–4745.

10. Verma, S., Kim, B., Jhong, H.R.M., Ma, S., and Kenis, P.J.A. (2016). A gross-margin model for defining technoeconomic benchmarks in the electroreduction of CO_2. ChemSusChem *9*, 1972–1979.

11. Ross, M.B., Dinh, C.T., Li, Y., Kim, D., De Luna, P., Sargent, E.H., and Yang, P. (2017). Tunable Cu enrichment enables designer syngas electrosynthesis from CO_2. J. Am. Chem. Soc. *139*, 9359–9363.

12. Sheng, W., Kattel, S., Yao, S., Yan, B., Liang, Z., Hawxhurst, C.J., Wu, Q., and Chen, J.G. (2017). Electrochemical reduction of CO_2 to synthesis gas with controlled CO/H_2 ratios. Energy Environ. Sci. *10*, 1180–1185.

13. He, R., Zhang, A., Ding, Y., Kong, T., Xiao, Q., Li, H., Liu, Y., and Zeng, J. (2018). Achieving the widest range of syngas proportions at high current density over cadmium sulfoselenide nanorods in CO_2 electroreduction. Adv. Mater. *30*, 1705872.

14. Kang, P., Chen, Z., Nayak, A., Zhang, S., and Meyer, T.J. (2014). Single catalyst electrocatalytic reduction of CO_2 in water to H_2 + CO syngas mixtures with water oxidation to O_2. Energy Environ. Sci. *7*, 4007–4012.

15. Liu, M., Pang, Y., Zhang, B., De Luna, P., Voznyy, O., Xu, J., Zheng, X., Dinh, C.T., Fan, F., Cao, C., et al. (2016). Enhanced electrocatalytic CO_2 reduction via field-induced reagent concentration. Nature *537*, 382–386.

16. Cave, E.R., Shi, C., Kuhl, K.P., Hatsukade, T., Abram, D.N., Hahn, C., Chan, K., and Jaramillo, T.F. (2018). Trends in the catalytic activity of hydrogen evolution during CO_2 electroreduction on transition metals. ACS Catal. *8*, 3035–3040.

17. Ruban, A.V., Skriver, H.L., and Nørskov, J.K. (1999). Surface segregation energies in transition-metal alloys. Phys. Rev. B *59*, 15990–16000.

18. Nilekar, A.U., Ruban, A.V., and Mavrikakis, M. (2009). Surface segregation energies in low-index open surfaces of bimetallic transition metal alloys. Surf. Sci. *603*, 91–96.

19. Yoo, J.S., Christensen, R., Vegge, T., Nørskov, J.K., and Studt, F. (2016). Theoretical insight into the trends that guide the electrochemical reduction of carbon dioxide to formic acid. ChemSusChem *9*, 358–363.

20. Hansen, H.A., Varley, J.B., Peterson, A.A., and Nørskov, J.K. (2013). Understanding trends in the electrocatalytic activity of metals and enzymes for CO_2 reduction to CO. J. Phys. Chem. Lett. *4*, 388–392.

21. He, J., Johnson, N.J., Huang, A., and Berlinguette, C.P. (2018). Electrocatalytic alloys for CO_2 reduction. ChemSusChem *11*, 48–57.

22. Lee, J.R.I., O'Malley, R.L., O'Connell, T.J., Vollmer, A., and Rayment, T. (2010). X-ray absorption spectroscopy characterization of Zn underpotential deposition on Au(111) from phosphate supporting electrolyte. Electrochim. Acta *55*, 8532–8538.

23. Venkatraman, K., Dordi, Y., and Akolkar, R. (2017). Electrochemical atomic layer deposition of cobalt enabled by the surface-limited redox replacement of underpotentially deposited zinc. J. Electrochem. Soc. *164*, D104–D109.

24. Herbert, J.J., Senecal, P., Martin, D.J., Bras, W., Beaumont, S.K., and Beale, A.M. (2016). X-ray spectroscopic and scattering methods applied to the characterisation of cobalt-based Fischer–Tropsch synthesis catalysts. Catal. Sci. Technol. *6*, 5773–5791.

25. Kornienko, N., Resasco, J., Becknell, N., Jiang, C.M., Liu, Y.S., Nie, K., Sun, X., Guo, J., Leone, S.R., and Yang, P. (2015). Operando spectroscopic analysis of an amorphous cobalt sulfide hydrogen evolution electrocatalyst. J. Am. Chem. Soc. *137*, 7448–7455.

26. Li, Y.C., Zhou, D., Yan, Z., Gonçalves, R.H., Salvatore, D.A., Berlinguette, C.P., and Mallouk, T.E. (2016). Electrolysis of CO_2 to syngas in bipolar membrane-based electrochemical cells. ACS Energy Lett. *1*, 1149–1153.

27. Verma, S., Hamasaki, Y., Kim, C., Huang, W., Lu, S., Jhong, H.R.M., Gewirth, A.A., Fujigaya, T., Nakashima, N., and Kenis, P.J.A. (2018). Insights into the low overpotential electroreduction of CO_2 to CO on a supported gold catalyst in an alkaline flow electrolyzer. ACS Energy Lett. *3*, 193–198.